

A Review of Red Sea Heat Flow

R. W. Girdler

Phil. Trans. R. Soc. Lond. A 1970 **267**, 191-203

doi: 10.1098/rsta.1970.0032

Email alerting service

Receive free email alerts when new articles cite this article - sign up in the box at the top right-hand corner of the article or click [here](#)

A review of Red Sea heat flow

BY R. W. GIRDLER

School of Physics, University of Newcastle upon Tyne

There are now twelve heat flow measurements in the Red Sea made with heat flow probes from survey ships and several sets of temperature measurements made in deep exploration boreholes.

The oceanic measurements are in water depths ranging from 0.94 to 2.70 km and all but one of these measurements give values significantly higher than the world mode of 46 mW m^{-2} (1.1).† They include the world record high oceanic measurement of more than 3307 mW m^{-2} (79.0) in the neighbourhood of the hot brine pools. These measurements show that the deep axial trough of the Red Sea is associated with high heat flow, the values being similar to those found in the mid-Indian Ocean rift, the mid-Atlantic rift and over the crest of the East Pacific rise.

It is of considerable interest to see if there is also high heat flow over the Red Sea margins and the main purpose of this paper is to examine temperature data from deep exploration boreholes. The boreholes are drilled mainly in rock salt, sandstones and shales. A discussion is given of the thermal conductivities assumed for these rocks. The boreholes have depths of up to 4 km and in some cases the temperature measurements enable an estimate to be made of the heat flow. These are also found to be high.

The significance of the high heat flow to ideas concerning the structure and evolution of the Red Sea is discussed.

INTRODUCTION

It is now well established that the world oceanic ridge-rift system is associated with high heat flow (Langseth, Le Pichon & Ewing 1966). The high heat flow occurs in a narrow belt, a few tens of kilometres wide and its location is closely associated with the location of the seismically active rift.

The Red Sea forms part of the world rift system and heat flow measurements in or near the deep, axial trough of the Red Sea by Sclater (1966), Birch & Halunen (1966), Langseth & Taylor (1967) and Erickson & Simmons (1969) give high values.

It is of interest to see how far the high heat flow extends over the Red Sea margins. As the water is too shallow in these regions to permit oceanic measurements, it is worthwhile to make a careful study of any temperature measurements which are available from exploration boreholes. The stratigraphical details of the boreholes cannot be disclosed but a good general picture of the marginal stratigraphy of the Red Sea is given by Heybroek (1965).

The heat flow is obtained by multiplying the thermal conductivity by the temperature gradient. Although borehole temperature measurements are available, there are no conductivity measurements. Conductivities have therefore to be estimated from the literature. Fortunately, the situation is helped by the fact that there are vast thicknesses of rock salt on the margins of the Red Sea. The rocks are otherwise sandstones and shales.

† In SI units (Système International), the unit of heat flow is joule per square metre per second ($\text{J m}^{-2} \text{s}^{-1}$) or watt per square metre (W m^{-2}). For terrestrial heat flow the most convenient unit is the milliwatt per square metre (mW m^{-2}). Since in the past nearly all terrestrial heat flow papers have used the microcalorie per square centimetre per second (sometimes called the heat flow unit, H.F.U.) this is given in parentheses. The conversion factor is $1 \text{ mW m}^{-2} = 2.389 \times 10^{-2} \mu\text{cal cm}^{-2} \text{s}^{-1}$.

THERMAL CONDUCTIVITIES

(a) *Rock salt*

The thermal conductivity varies with temperature and pressure and as some of the boreholes have depths of nearly 4 km it is necessary to see if these effects are significant.

Experimental data for the thermal conductivity of rock salt were taken from the *Handbook of physical constants* (Birch & Clark 1966) for the temperature range of interest $0 \leq \theta \leq 200$ °C. These are shown in figure 1. As the temperature range is a small one, a least squares straight line was fitted. The conductivity k ($\text{W m}^{-1} \text{K}^{-1}$) is related to the temperature θ (°C) by

$$k = -(0.015 \pm 0.005)\theta + (5.996 \pm 0.309)$$

for $0 \leq \theta \leq 200$ °C.

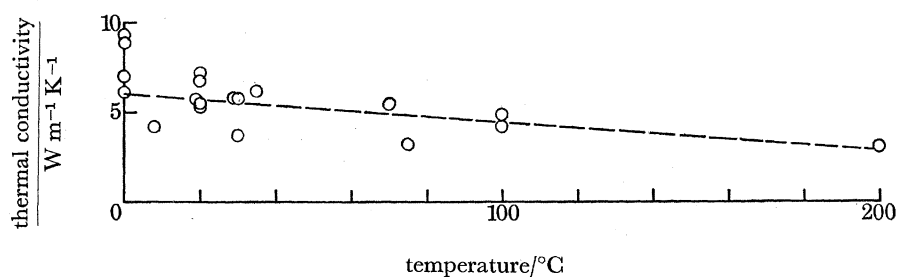


FIGURE 1. Variation of thermal conductivity with temperature for rock salt.

Theoretically, the thermal conductivity is inversely proportional to the absolute temperature and Birch & Clark (1940) have shown this to be so for rock salt for the temperature interval $0 \leq \theta \leq 400$ °C. For the smaller temperature range of interest here, there is little difference between the two relations and the above equation which includes the latest experimental data is used.

There is a small effect due to hydrostatic pressure given by

$$k = k_0(1 + \alpha P),$$

where k_0 is the conductivity at normal pressure and $\alpha = 3.6 \times 10^{-5}$ when P is in kg cm^{-2} (Clark 1966). The effect increases the conductivity by a small percentage over the ranges of depth considered.

(b) *Sandstones and shales*

For some of the Red Sea boreholes, the stratigraphic logs list undifferentiated sandstones and shales. The mean thermal conductivity for sandstones and shales from Clark (1966) is $2.628 \pm 0.301 \text{ W m}^{-1} \text{K}^{-1}$ (17 sets of data). The data cover a wide range of values and in general, sandstones have higher conductivity than shales. The mean conductivity for sandstones is $3.093 \pm 0.393 \text{ W m}^{-1} \text{K}^{-1}$ (11 sets of data) and for shales $1.779 \pm 0.142 \text{ W m}^{-1} \text{K}^{-1}$ (6 sets of data). A further difficulty is the water content of the sediments. The difference in conductivity for some sandstones in the dry and wet state can be as high as 65%. For the deep boreholes discussed here, the best that can be done is to use the mean ($2.628 \text{ W m}^{-1} \text{K}^{-1}$) of all value listed.

RED SEA HEAT FLOW

193

TEMPERATURE GRADIENTS AND HEAT FLOW FOR DEEP BOREHOLES

Red Sea boreholes for which useful temperature data are available are considered from north to south.

(a) *Durwara 1 and 2*

These two boreholes are close together on the western margin of the Red Sea at latitude 18.81° N, longitude 37.64° E. The geological strata consists of salt and sandstones and shales (Baldassarri 1967).

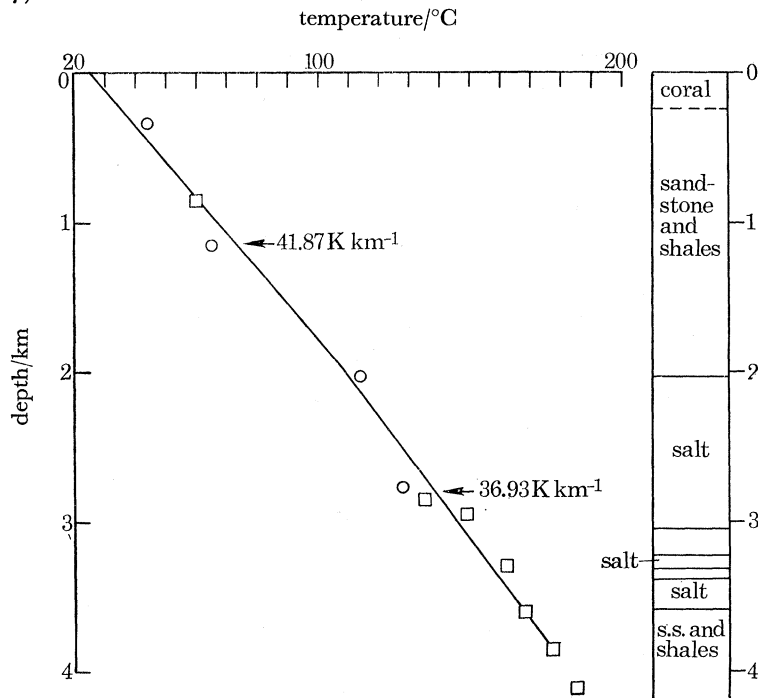


FIGURE 2. Temperatures for the boreholes Durwara 1 (○) and Durwara 2 (□) (latitude 18.81° N, longitude 37.64° E).

TABLE 1. DURWARA 1 AND 2

approx. depth/km	rock strata	temp. gradient K km^{-1}	conductivity $\text{W m}^{-1} \text{K}^{-1}$	heat flow mW m^{-2} ($\mu\text{cal cm}^{-2} \text{s}^{-1}$)
0 to 2	sands and shales	41.87	2.628	110 (2.63)
2 to 3.5	salt	36.93	3.872	143 (3.42)
				mean 126 (3.02)

Four bottom-hole temperature measurements were made in borehole 1 and seven in borehole 2. As the wells are close together, the data have been combined to obtain the temperature-depth curves shown in figure 2. Least squares straight line relations were obtained for depth d (km) and temperature θ ($^\circ\text{C}$) for the two sets of rock strata. These are:

$$d = (41.87 \pm 3.82)\theta + (25.04 \pm 4.27) \quad \text{for sands and shales,}$$

$$d = (36.93 \pm 5.66)\theta + (34.93 \pm 16.75) \quad \text{for salt.}$$

The errors for the temperature gradients are of the order of 10 and 15% respectively. Assuming values for the conductivities from the previous section, the heat flows corresponding to these gradients were obtained and are given in table 1. The mean heat flow is 126 mW m^{-2}

(3.0). The errors in the gradients, together with the uncertainties in the conductivity estimates, suggest this value maybe in error by 30 to 40 %. Even so, it is significantly higher than the world mean.

(b) *Mansiyah 1*

This borehole is located on the eastern margin of the Red Sea at latitude 17.22° N, longitude 42.37° E. The geologic column consists of over 1.2 km of rock salt overlain and underlain by sandstones and shales (Gilman 1969).

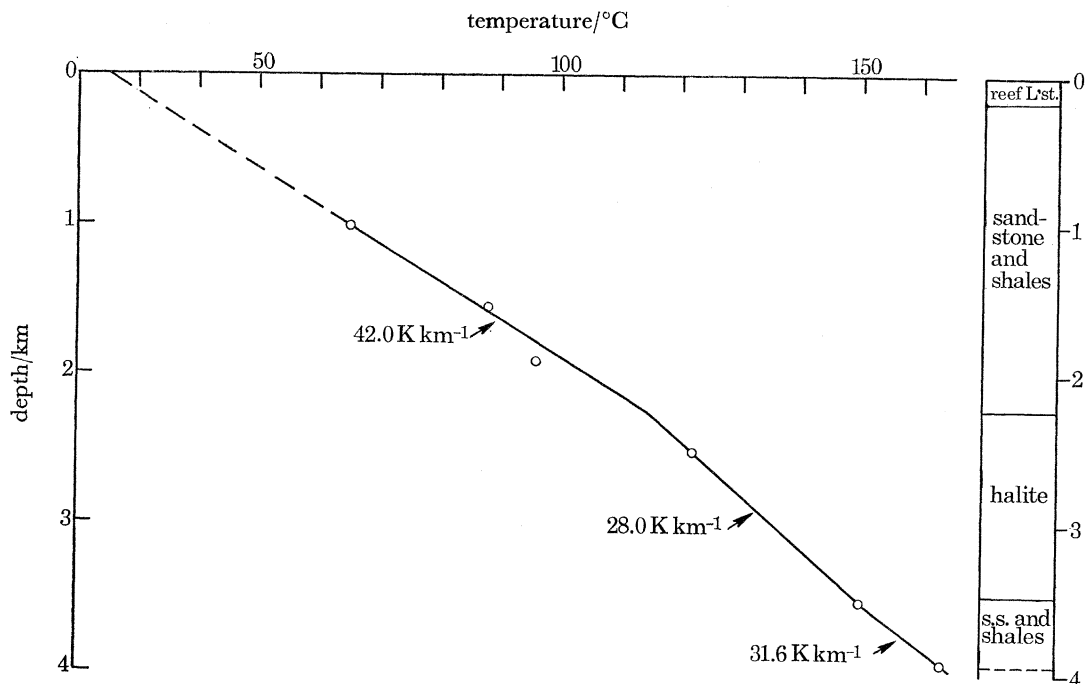


FIGURE 3. Temperatures for the borehole Mansiyah 1 (latitude 17.22° N, longitude 42.37° E).

TABLE 2. MANSIYAH 1

approx. depth/km	rock strata	temp. gradient K km ⁻¹	conductivity W m ⁻¹ K ⁻¹	heat flow mW m ⁻² (μcal cm ⁻² s ⁻¹)
1.0 to 2.0	sands and shales	42.0	2.628	110 (2.64)
2.0 to 3.5	rock salt	28.0	4.022	113 (2.69)
				mean 111 (2.67)

There are six bottom-hole temperature measurements: 65 °C at 1.010 km, 88 °C at 1.555 km, 96 °C at 1.912 km, 122 °C at 2.514 km, 150 °C at 3.514 km and 163 °C at 3.926 km giving the temperature–depth curves of figure 3. From these data, it is possible to estimate two temperature gradients; 42.0 K km⁻¹ for the sands and shales and 28.0 K km⁻¹ for the rock salt. These give the heat flow values of table 2. It is seen that the heat flow for the two sets of rock strata are in good agreement. This, together with the fact that the temperature gradient gives a reasonable value for the surface temperature on extrapolation (26 °C) suggests that a value of 111 mW m⁻² (2.67) is probably a good estimate for the heat flow in this borehole.

(c) Amber 1

This borehole is located on the southwest margin of the Red Sea and has coordinates 16.35° N, 40.01° E. The geological column is mainly rock salt.

Three bottom-hole temperatures were measured at 0.917, 2.567 and 3.551 km. The temperatures were 60.0, 101.7 and 130 °C. respectively. The measurements were made using a Schlumberger borehole compensated sonic sonde in a salt-saturated drilling fluid approximately 12 h after drilling ceased. According to Bullard (1947) the temperature just at the bottom of the

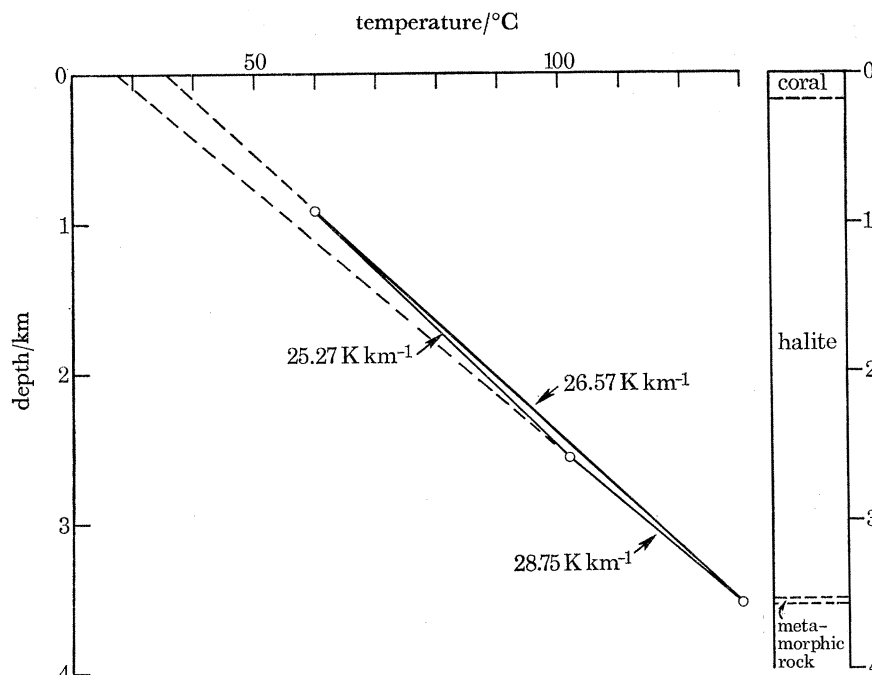


FIGURE 4. Temperatures for the borehole Amber 1 (latitude 16.35° N, longitude 40.01° E).

TABLE 3. AMBER 1

depth/km	temp. gradient	k (rock salt)	heat flow
	$K km^{-1}$	$W m^{-1} K^{-1}$	$mW m^{-2} (\mu cal cm^{-2} s^{-1})$
0.917 to 2.567	25.27	4.794	121 (2.89)
2.567 to 3.551	28.75	4.282	123 (2.94)
0.917 to 3.551	26.57	4.586	122 (2.91)
			mean 122 (2.91)

hole should have recovered from the cooling effect of the drilling fluid in this time. The temperatures are therefore assumed to be equilibrium temperatures. Three temperature gradients may be calculated (figure 4) and these are 25.27, 28.75 and 26.57 $K km^{-1}$. The surface extrapolated temperatures (figure 4) are somewhat high. This is probably entirely due to the presence of about 0.2 km of low conductivity coral overlying the rock salt.

Heat flow values have been calculated for the three temperature gradients and are given in table 3. The thermal conductivities were computed for the temperatures and pressures corresponding to depths half way between the temperature measurements using the relations given above. The three values of heat flow so obtained are in close agreement (table 3) and give a

mean of 122 mW m^{-2} (2.92) with a standard deviation of less than 1%. The agreement is probably fortuitous as there are only three temperature measurements. It is difficult to estimate a realistic error for this heat flow but the combined error for gradient and conductivity probably does not exceed $\pm 20\%$.

(d) *Dhunishub 1*

This borehole is located on the southwest margin of the Red Sea at latitude 15.72° N , longitude 40.62° E and is mostly through rock salt.

Three bottom temperatures were measured: 72.2° C at 0.915 km, 82.2° C at 1.951 km and 171.1° C at 3.865 km. The second measurement was made soon after circulation ceased and is considered unreliable. The first measurement was made 10.5 h and the last 48 to 72 h after circulation ceased. These measurements are probably reliable, especially the last.

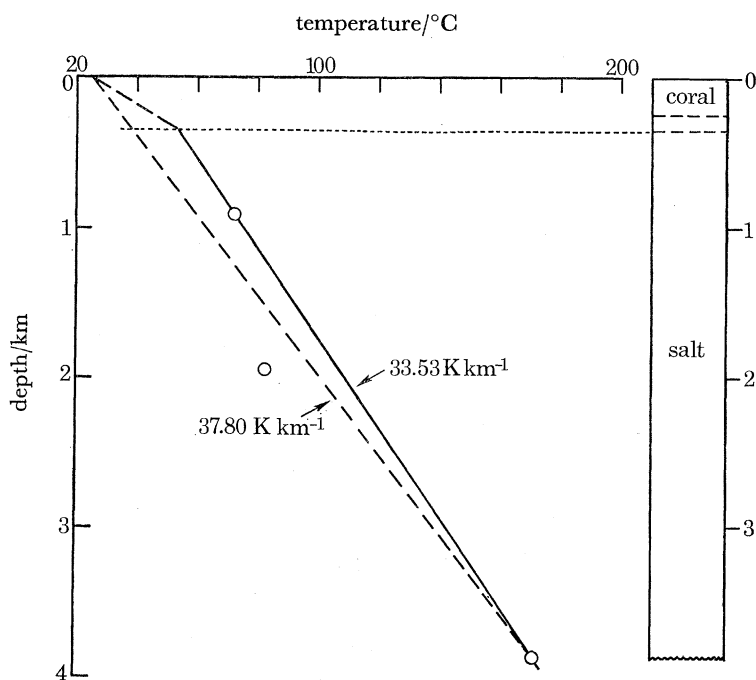


FIGURE 5. Temperatures for the borehole Dhunishub 1 (latitude 15.72° N , longitude 40.62° E).

Figure 5 shows the probable temperature–depth curve (solid line) with maximum weight attached to the temperature measurements at 0.915 and 3.865 km. These give a temperature gradient of 33.53 K km^{-1} . A linear extrapolation of this curve to zero depth gives 42° C which is somewhat high as a surface (sea) temperature of 25 to 30° C is to be expected. This is probably due to the presence of low conductivity coral in the top 0.35 km of the section. Assuming the temperature curve in figure 5, the gradient for the top 0.35 km is 83 K km^{-1} implying an average thermal conductivity of about $1.7 \text{ W m}^{-1} \text{ K}^{-1}$ which is not unreasonable for coral. The heat flow calculated for the temperature gradient through the rock salt is 140 mW m^{-2} (3.35).

A maximum estimate of the heat flow maybe obtained by assuming a surface temperature of 25° C and the deepest temperature measurement (made 48 to 72 h after drilling ceased) to

be wholly reliable. The average temperature gradient (dashed line in figure 5) is then 37.80 K km^{-1} giving a heat flow of 168 mW m^{-2} (4.03). The data are summarized in table 4.

In addition to the bottom measurements, a Schlumberger temperature log is available for this borehole. Temperatures were read at 0.1 km depth intervals from the continuous log and a least squares straight line fitted. The gradient was found to be $20.97 \pm 0.15 \text{ K km}^{-1}$, i.e. considerably less than that calculated from the bottom temperatures. To further investigate the reliability of the log, the temperature gradient (second derivative) was calculated for each 0.1 km depth interval. This was found to decrease slightly with depth instead of increasing to compensate for the decrease of thermal conductivity of rock salt with increasing temperature. It was therefore concluded that the log could not be used.

TABLE 4. DHUNISHUB 1

depth/km	temp. gradient	k (rock salt)	heat flow
	K km^{-1}	$\text{W m}^{-1} \text{K}^{-1}$	$\text{mW m}^{-2} (\mu\text{cal cm}^{-2} \text{s}^{-1})$
0.915 to 3.865	33.53	4.183	140 (3.35)
0.354 to 3.865	37.80	4.458	168 (4.03)

The best estimate for the heat flow is probably 140 mW m^{-2} (3.35) which may be in error by as much as 40 %, the temperature gradient being in error by a possible 25 % and the thermal conductivity by a possible 15 %.

(e) *Secca Fawn 1*

This borehole is also located on the southwest margin of the Red Sea and has coordinates 15.39° N , 40.16° E . The site is nearer the coast and the boring passed through much less evaporite and many more gravels, sands and clays making the estimation of thermal conductivities more difficult.

Temperature measurements were made at depths of 1.030, 2.627 and 2.665 km. The deepest measurement which gave 166° C was made 43 h after drilling ceased and is considered reliable. At 2.627 km, four measurements were made at 7, 11, 19 and 24 h after drilling ceased giving a temperature equilibrium curve from which a temperature of 165° C can be estimated for this depth. At 1.030 km a temperature of 66° C was measured 8 h after drilling ceased; if it is assumed that the borehole attained equilibrium along a similar curve to that for 2.627 km depth, an equilibrium temperature of about 101° C is obtained. In addition, Scorcelletti (personal communication) estimated a temperature of 193° C at 3.363 km (the bottom of the hole) from flow line temperatures. These temperatures are plotted in figure 6.

From figure 6, it is possible to obtain two useful temperature gradients. First, below about 3.3 km, there is rock salt for which the temperature gradient is 36.51 K km^{-1} ; the thermal conductivity of salt for these pressure and temperature conditions is $3.326 \text{ W m}^{-1} \text{K}^{-1}$ giving a heat flow of 121 mW m^{-2} (2.90). Secondly, using the estimated temperature of 101° C at 1.030 km the temperature gradient for the overlying detrital sediments is 41.76 K km^{-1} . As the sediments consist mainly of clays, siltstones, sands and gravels with only a thin layer of evaporites at about 1.2 to 1.3 km the mean conductivity for sandstones from § 2 is used giving a heat flow of 129 mW m^{-2} (3.09). The mean heat flow for the two sets of strata is therefore 125 mW m^{-2} (2.99) and the error is probably similar to that for the Dhunishub 1 borehole.

A maximum estimate for the heat flow in this well maybe obtained by assuming a surface sea temperature of 25° C and the temperatures at 2.627 and 2.665 km to be wholly reliable

(dashed line in figure 6). Assuming the same value for the thermal conductivity of the detrital sediments this gives a heat flow of 165 mW m^{-2} (3.91). The estimates are summarized in table 5.

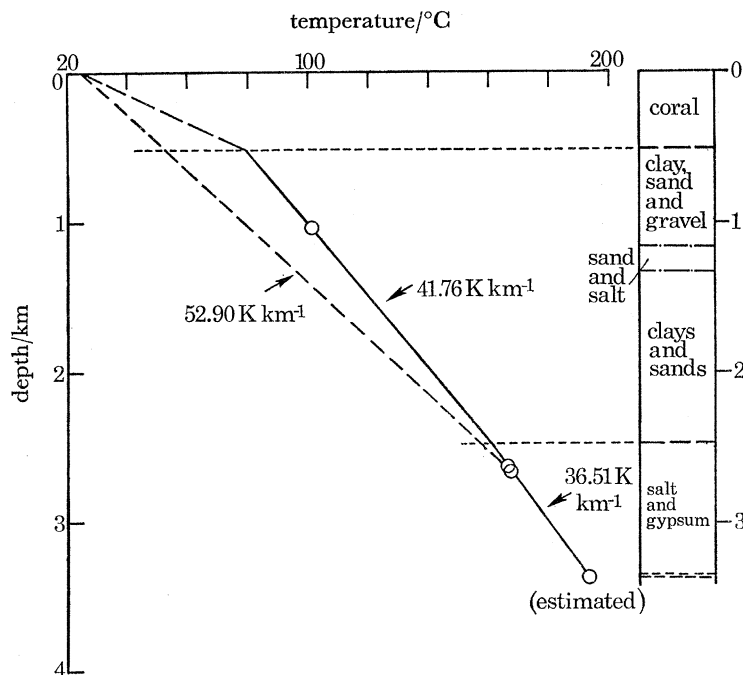


FIGURE 6. Temperatures for the borehole Secca Fawn I (15.39° N , 40.16° E).

TABLE 5. SECCA FAWN I

approx. depth/km	rock strata	temp. gradient K km^{-1}	conductivity $\text{W m}^{-1} \text{K}^{-1}$	heat flow mW m^{-2} ($\mu\text{cal cm}^{-2} \text{s}^{-1}$)
0.5 to 2.5	shales, sands, etc.	41.76	3.093	129 (3.09)
2.5 to 3.4	salt	36.51	3.326	121 (2.90)
				mean 125 (2.99)
0 to 2.7	shales, sands, etc.	52.90	3.093	max 164 (3.91)

SUMMARY OF HEAT FLOW DATA

All heat flow measurements available to March 1969 are summarized in table 6 where they are arranged by decreasing latitude.

From the data available (figure 7) it seems that the whole of the Red Sea is associated with high heat flow, all but one value being higher than the world mean. The values for the four deep wells along the western margin of the Red Sea (126 , 122 , 140 and 125 mW m^{-2}) and the one value on the eastern margin (111 mW m^{-2}) are remarkably consistent indicating that the high heat flow extends to the sides. It is unfortunate that there are no measurements on land so that the width of the high heat flow zone can be demarcated. The region of high heat flow over the mid-Atlantic ridge (Langseth *et al.* 1966) is confined to a crestal zone not more than 200 km wide. It seems likely that the high heat flow over the Red Sea is confined to the main Red Sea depression.

Figure 8 shows the heat flow values plotted as a function of distance from the axis of the Red

RED SEA HEAT FLOW

199

Sea. The few values which are available indicate that the highest heat flow is over the centre and there is a decrease with distance from the axis similar to that found over the mid-Indian Ocean rift, the mid-Atlantic rift and the East Pacific rise (McKenzie 1967). Figure 9 shows for comparison the heat flow over the mid-Indian Ocean ridge.

TABLE 6. SUMMARY OF HEAT FLOW MEASUREMENTS

	latitude (°N)	longitude (°E)	water depth km	heat flow		reference
				mW m ⁻²	(μ cal cm ⁻² s ⁻¹)	
Co 9-113	25.47	35.49	1.335	267	(6.37)	Langseth & Taylor (1967)
CH 43-24	25.40	36.17	2.205	\geq 96	(2.29)	Birch & Halunen (1966)
CH 61-167	23.33	37.33	0.826	176	(4.20)	Erickson & Simmons (1969)
CH 61	21.37	38.08	\approx 2.0	$>$ 3306	(79.0)	Erickson & Simmons (1969)
5234	20.45	37.92	0.870	?134	(3.20)	Slater (1966)
CH 61-153	19.72	38.68	2.704	335	(8.01)	Erickson & Simmons (1969)
CH 61-154	19.57	38.98	1.276	107	(2.55)	Erickson & Simmons (1969)
CH 61-155	19.38	38.90	2.207	63	(1.5)	Erickson & Simmons (1969)
Durwara 1, 2	18.81	37.64	shelf	126	(3.02)	this paper
5232	18.40	39.78	1.480	44	(1.06)	Slater (1966)
Mansiyah 1	17.22	42.37	shelf	111	(2.67)	this paper
Amber 1	16.35	40.01	shelf	122	(2.91)	this paper
Co 9-112	16.34	40.47	1.223	90	(2.16)	Langseth & Taylor (1967)
Co 9-111	16.22	41.21	0.941	180	(4.30)	Langseth & Taylor (1967)
5231	15.97	41.52	1.735	175	(4.18)	Slater (1966)
Dhunishub 1	15.72	40.62	shelf	140	(3.35)	this paper
Secca Fawn 1	15.39	40.16	shelf	125	(2.99)	this paper

SIGNIFICANCE OF RESULTS

The high heat flow over the Red Sea is to be expected in view of the presence of an intrusive zone. There is now abundant evidence summarized in Girdler (1969) that the Red Sea has formed by the separation of Arabia away from Africa. A vital piece of evidence is the presence of large magnetic anomalies and their interpretation by Vine (1966). Vine has been able to show that the Red Sea has been opening at a spreading rate of about 1 cm a⁻¹ per flank over the last 4 Ma. The seismicity (Fairhead & Girdler, this volume, p. 49) suggests that the separation is still going on and new material is being injected beneath the centre. McKenzie (1967) has calculated the heat flow to be expected in a region of spreading when the plates are of constant thickness and are moving at a constant velocity. The width and shape of the heat flow anomaly are controlled mainly by the spreading rate. Figure 8 shows the theoretical heat flow anomaly when a 50 km thick plate moves at constant velocities of 1 and 2 cm a⁻¹ respectively. As for the mid-Atlantic and mid-Indian Ocean ridges and East Pacific rise (McKenzie 1967) this simple model fits the data remarkably well.

Near the axis, the heat flow is likely to be variable and controlled by details of the shape and size of the intrusion. Unfortunately, there is still insufficient geophysical data to give fine details of the intrusive zone. The total separation may be estimated from the 100 km displacement observed by Quennell and Freund along the Dead Sea-Jordan rift and the 7° anticlockwise rotation of Arabia with respect to Africa (Girdler 1966). The widths with topographic profiles for various latitudes are shown in figure 10. The nature of the topography is discussed more fully in Drake & Girdler (1964) and Girdler (1969).

In the north, the topography is relatively simple with the main trough having fairly uniform water depth of about 1 km. So far, no evidence has been obtained for actual separation of the

crust in this part of the Red Sea. The Bouguer gravity anomaly is only +600 g.u.* compared with +1200 to +1500 g.u. farther south, and the two seismic refraction profiles give velocities of 5.8 to 5.9 km s⁻¹ indicating the presence of Precambrian shield rocks. As the 100 km horizontal displacement along the Aqaba–Dead Sea rift must affect the northern part of the Red Sea there must be strong plate attenuation as shown diagrammatically in the top sections of figure 11. The heat flow would be high over such a structure due to the intrusive zone being close to the surface.

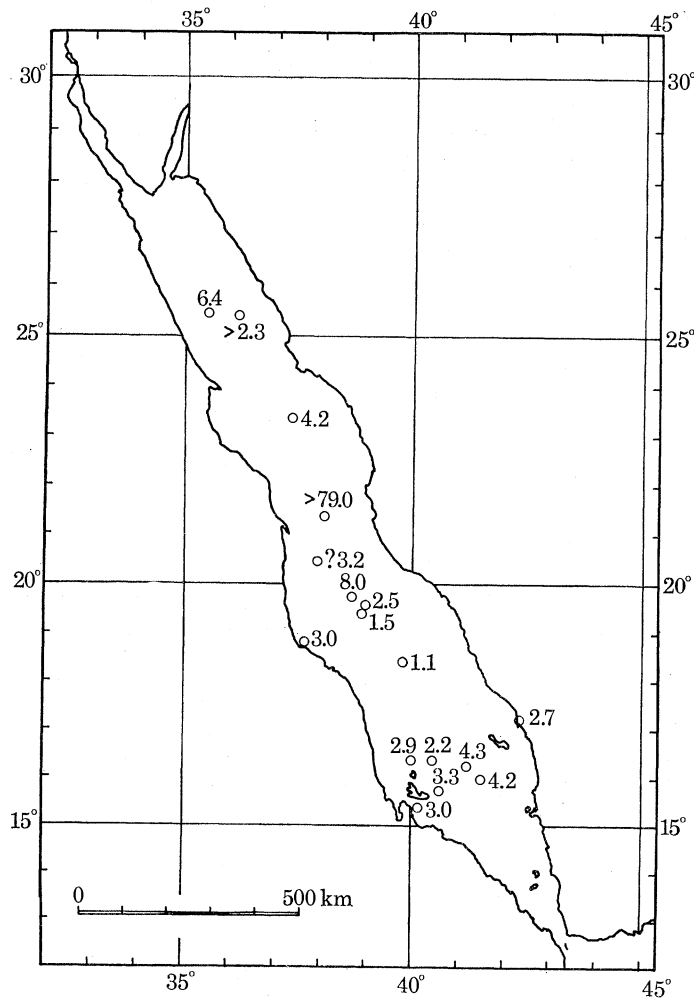


FIGURE 7. Heat flow measurements available for the Red Sea as at March 1969. The units are $\mu\text{cal cm}^{-2} \text{s}^{-1}$ ($1 \mu\text{cal cm}^{-2} \text{s}^{-1} = 41.855 \text{ mW m}^{-2}$).

At about 24° N, a deep, axial trough begins to develop and widens towards the south. The largest magnetic anomalies, the newest crust and the highest heat flow (figure 8) are associated with this axial trough.

In the south (e.g. the profile for 16.5° N figure 10), the structure is obscured by large thicknesses of sediments, especially evaporites. These extend from the margins and in the extreme south reach nearly to the centre of the Sea. In this region, the seismicity and magnetic anomalies suggest there may be more than one region of crustal separation. The situation is depicted diagrammatically in the lower two sections of figure 11. This could account for the high heat

* 1 gravity unit (g.u.) = 10^{-5} m s^{-2} .

RED SEA HEAT FLOW

201

flow on the south west margin of the Red Sea; the three values being considerably higher than expected (figure 8).

Figure 11 shows the possible nature of the progressive development of the Red Sea from north to south. The near surface P wave velocity of the continental crustal material is $5.9 \pm 0.2 \text{ km s}^{-1}$ and of the oceanic material $7.1 \pm 0.2 \text{ km s}^{-1}$. The latter probably increases to about 8 km s^{-1} beneath the shield rocks under the plateau on either side.

The separation has been taking place in phases, either in the form of attenuation or dyke injection over the last 30 Ma. Crustal separation in the form of sea floor spreading has been going on over the last 4 Ma and possibly over the last 10 Ma.

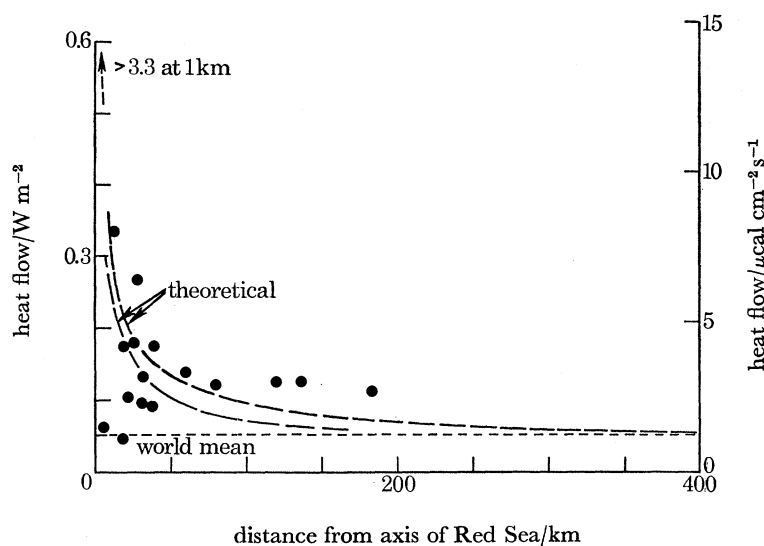


FIGURE 8. Heat flow plotted as a function of distance from the axis of the Red Sea. Theoretical curves (after McKenzie 1967) are for a 50 km thick plate moving with a velocity of 1 cm a^{-1} (lower curve) and 2 cm a^{-1} (upper curve).

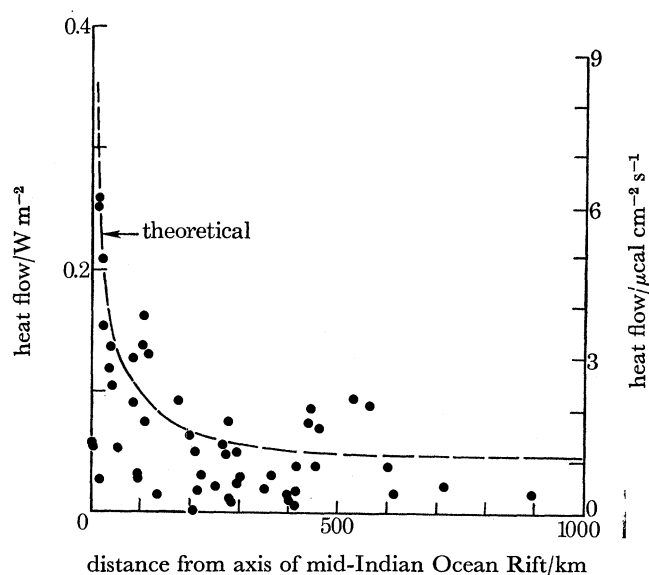


FIGURE 9. Heat flow values plotted as a function of distance for the mid-Indian Ocean ridge for comparison with figure 8. The theoretical curve is for a spreading rate of 2 cm a^{-1} (after McKenzie 1967).

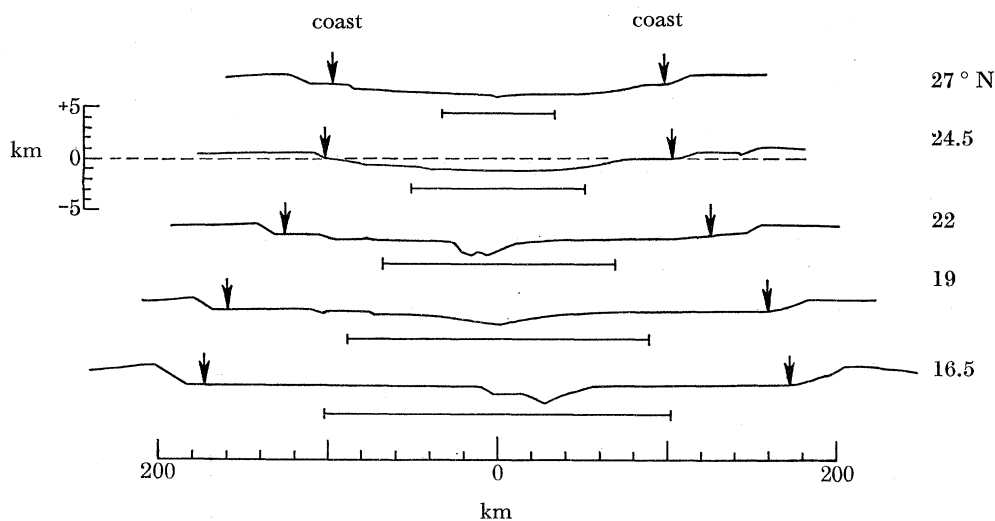


FIGURE 10. Topographic profiles taken at right angles to the axis of the Red Sea (from the bathymetric charts of Laughton 1968). The vertical exaggeration is 6:1. The distances beneath each profiles are for the crustal separation to be expected assuming a horizontal displacement of 100 km along the Dead Sea–Aqaba rift.

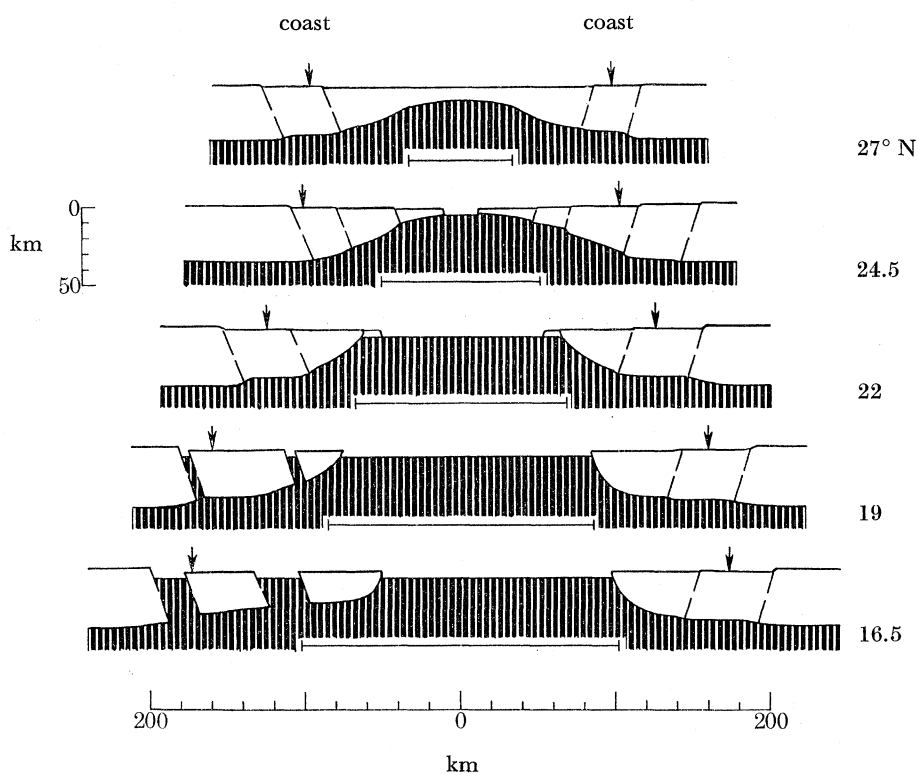


FIGURE 11. Possible structures (vertical scale = horizontal scale) for the profiles of figure 10 based on the horizontal displacement along the Dead Sea–Aqaba rift and consistent with gravity anomalies and seismic refraction profiles. The profiles are diagrammatic and the surface geology is omitted. The secondary areas of crustal separation on the western margin could explain the presence of high heat flow and volcanicity in this region.

CONCLUSIONS

Temperature measurements in deep boreholes can give useful estimates of heat flow even if the estimates maybe in error by up to 30 to 40 %. Measurements in five deep boreholes near the margins of the Red Sea give heat flow values significantly higher than the world mean. The Red Sea is like other parts of the world rift system in having high heat flow, the highest heat flow being along the axis where the newest crust is being injected along seismically active zones. The heat flow distribution is consistent with that to be expected from the break up of a rigid plate (Africa and Arabia) and its subsequent moving apart.

I am most grateful to the Gulf, Mobil and Auxerap Oil Companies for releasing the data used in this paper and in particular to S. B. Frazier and P. G. Scorcelletti (Gulf), J. Kingston, G. Engels, R. Olson and G. Gibson (Mobil) and M. Gilman (Auxerap). I am also grateful to Sir Edward Bullard, F.R.S., Professor Gene Simmons and Professor R. Von Herzen for helpful discussions during the early phases of this work.

REFERENCES (Girdler)

- Baldassarri, G. 1967 Trouble's triplets. *Drilling*, pp. 88–91.
- Birch, F. & Clark, H. 1940 The thermal conductivity of rocks and its dependence on temperature and pressure. *Am. J. Sci.* **238**, 529–558.
- Birch, F. S. & Halunen, A. J. 1966 Heat flow measurements in the Atlantic Ocean, Indian Ocean, Mediterranean Sea and Red Sea. *J. geophys. Res.* **71**, 583–586.
- Bullard, E. C. 1947 The time necessary for a bore hole to attain temperature equilibrium. *Mon. Not. R. astr. Soc. geophys. Suppl.* **5**, 127–130.
- Clark, S. P. 1966 Thermal conductivity. *Handbook of physical constants*. (revised edn). *Geol. Soc. Am. Mem.* **97**, 459–482.
- Drake, C. L. & Girdler, R. W. 1964 A geophysical study of the Red Sea. *Geophys. J. R. astr. Soc.* **8**, 473–495.
- Erickson, A. J. & Simmons, G. 1969 Thermal measurements in the Red Sea hot brine pools. In *Hot brines and recent heavy metal deposits in the Red Sea*, pp. 114–121 (Degens, E. T. and Ross, D. A., eds.). New York: Springer-Verlag.
- Gilman, M. 1969 Primary results of a geological and geophysical reconnaissance of the Jizan coastal plain of Saudi Arabia. *Second Reg. Tech. Symp. Soc. Petrol. Engng AIME, Saudi Arabia Section, Dhahran*.
- Girdler, R. W. 1958 The relationship of the Red Sea to the East African Rift System. *Q. Jl geol. Soc., Lond.* **114**, 79–105.
- Girdler, R. W. 1966 The role of translational and rotational movements in the formation of the Red Sea and Gulf of Aden. In *The World Rift System, Geol. Surv. Pap. Can.* **66-14**, 65–75.
- Girdler, R. W. 1969 The Red Sea—a geophysical background. In *Hot brines and recent heavy metal deposits in the Red Sea*, pp. 38–58 (Degens, E. T. and Ross, D. A., eds.). New York: Springer-Verlag.
- Heybroek, F. 1965 The Red Sea Miocene Evaporite Basin. In *Salt Basins around Africa*, 17–40. London: Institute of Petroleum.
- Langseth, M. G., Le Pichon, X. & Ewing, M. 1966 Crustal structure of mid-oceanic ridges. 5. Heat flow through the Atlantic ocean floor and convection currents. *J. geophys. Res.* **71**, 5321–5355.
- Langseth, M. G. & Taylor, P. T. 1967 Recent heat flow measurements in the Indian Ocean. *J. geophys. Res.* **72**, 6249–6260.
- McKenzie, D. P. 1967 Some remarks on heat flow and gravity anomalies. *J. geophys. Res.* **72**, 6261–6273.
- Sclater, J. G. 1966 Heat flow in the north west Indian Ocean and Red Sea. *Phil. Trans. Roy. Soc. Lond.* A **259**, 271–278.
- Vine, F. J. 1966 Spreading of the ocean floor: new evidence. *Science, N.Y.* **154**, 1405–1415.